Mater. Res. Soc. Symp. Proc. Vol. 844 © 2005 Materials Research Society Y9.9.1

Mechanical Behavior of Ceramic/SAM Bilayer Coatings

Quan Yang, Guangneng Zhang, Kaustubh Chitre and Junghyun Cho
Department of Mechanical Engineering
State University of New York at Binghamton
Binghamton, NY 13902, U.S.A.

ABSTRACT

Ceramic/self-assembled monolayer (SAM) bilayer films can provide adequate protection and/or act as a multipurpose coating for microelectronics and MEMS applications, due to synergistic effects of the hybrid film structure. The organic SAM acts as a "template" for the growth of the ceramic film while the hard ceramic can provide protection from environmental and mechanical impact. To process the bilayer films, a low-temperature solution deposition technique (biomimetic process) is employed using phosphonate-based SAM and zirconium oxide precursors. A particulate zirconium oxide film is formed by enhanced hydrolysis of zirconium sulfate solutions in the presence of HCl at about 80°C, and its particle size and thickness effects are discussed. In addition, microstructure and micromechanics involved in the synthesis of both zirconia films and SAM are systematically assessed. Especially, mechanical properties such as Young's modulus and hardness are analyzed using a nanoindenter, as well as with the aid of theoretical models. Further, the substrate effects resulting from a large indentation depth relative to the film thickness are eliminated to obtain the "film-only" properties. This study also highlights the role of compliant SAM layer in forming a strain-tolerant bilayer film.

INTRODUCTION

A common issue of MEMS is the need for hermetic packaging in order to isolate and protect the device against adverse environmental effects. Hermetic packaging, however, not only increases the size of a MEMS device, but also raises the cost. In addition, proper surface modifications are essential for specific MEMS applications [1]. One sensible way to tackle these problems is to produce robust surface coatings on the surface of silicon. Such features would in turn benefit the MEMS packaging development by relaxing the stringent requirements for the assembly, thereby drastically reducing the packaging cost. Ceramics, due to good mechanical and thermal properties, are good candidate materials for surface coatings. However, the major challenge to producing ceramic films on silicon is to avoid the brittleness such as crack formation and spallation of the films while having a capability to process at low temperatures.

In an attempt to grow the strain-tolerant ceramic films, self-assembled monolayer (SAM) with phosphonate surface functionalities is pre-deposited on single-crystal silicon substrates. This self-assembly technique has been used to grow an organic monolayer on the Si/SiO_2 substrate [2-5]. The underlying SAM acts as an organic template for the subsequent growth of ceramic film, as well as a buffer layer to relieve the stress in the ceramic film. This process copies the biomineralization of inorganic (ceramic) materials frequently found in biological environments (called 'biomimetic' process). In this study, zirconium oxide films were formed on the SAM-coated silicon wafers by enhanced hydrolysis of zirconium sulfate ($Zr(SO_4)_2 \cdot 4H_2O$) solutions in acid environment at 80°C. One purpose of this study is to develop a bilayer structure that employs the advantages of organic SAM while processing hard and stiff inorganic protective

films. Such bilayer syntheses were previously reported in the literature but they all utilize the sulfonate terminated SAM with a $Zr(SO_4)_2 \cdot 4H_2O$ precursor [6-8]. In addition, there is no systematic study on mechanical performance. We herein report the synthesis of the bilayer films and corresponding microstructure and mechanical properties.

EXPERIMENTAL PROCEDURE

The substrates used in this study were n-type (100) single crystal silicon wafers (Silicon Quest International, Santa Clara, CA). They were cut into ca. 1cm x 1cm samples. The silicon wafers were then ultrasonically cleaned in acetone, and then cleaned by freshly prepared piranha solution (1 part 30% H_2O_2 + 3 parts 98% H_2SO_4) for 30 min. The wafers were then rinsed with deionized water and dried with a nitrogen stream. The cleaned silicon wafers were soaked into trichlorosilane or triethoxysilane solutions in a vacuum-sealed cell or a glove box for 24 hours. In this study, we focused on diethylphosphatoethyltriethoxysilane ($C_{12}H_{29}O_6PSi$, Gelest Inc., Tullytown, PA), which reacts with silicon oxide and forms a SAM on the silicon surface (denoted as "PO-SAM"). The PO-SAM, whose surface functionality was $PO(OC_2H_5)_2$— in the as-deposited state, was further hydrolyzed in 1-M HCl solution at 80°C for 30 min to obtain a suitable surface functionality ($PO(OH)_2$—) for the subsequent ceramic deposition.

Ceramic deposition was carried out through a near-room temperature aqueous solution process. A freshly prepared 0.01-M zirconium sulfate ($Zr(SO_4)_2 \cdot 4H_2O$, Alfa Aesar, Ward Hill, MA) + 0.4-M HCl aqueous solution was used. The PO-SAM coated Si wafers were soaked in this solution at 80°C for different durations: 0.5-hr, 5-hr, 20-hr and 24-hr. After each duration was reached, the wafer was taken out, rinsed with deionized water, and dried in a nitrogen stream.

Mechanical properties of the ceramic films, specifically Young's modulus (E_r) and hardness (H), were measured by a nanoindenter (TriboScope®, Hysitron Inc., Minneapolis, MN) which has a built-in atomic force microscope (AFM). Reduced Young's modulus E_r is related to the actual modulus of the film as given by

$$\frac{1}{E_r} = \left(\frac{1-\nu^2}{E}\right)_{film} + \left(\frac{1-\nu^2}{E}\right)_{indenter} \quad (1)$$

where E and ν are the Young's modulus and Poisson's ratio, respectively. The modulus of the indenter for our instrument is 1140 GPa, and Poisson's ratio is 0.07. The hardness H has the normal definition as given by

$$H = \frac{P_{\max}}{A} \quad (2)$$

where $P_{\max}$ is the maximum indentation load and A is the projected contact area at that load.

The sample with a 24-hr ceramic deposition was further annealed to 200°C, 500°C, 800°C, 1000°C, and 1200°C in an attempt to explore the structural evolution. Mechanical properties were measured at each annealing step.

RESULTS AND DISCUSSION

The ZrO_2 film growth mechanisms were studied by examining samples immersed in solution at different times, i.e., 0.5 hour, 5 hours, 20 hours and 24 hours. Microstructure of the film

resembles a particulate structure, as shown in the AFM images (Fig. 1). There was very little deposition on the 0.5-hr sample, wherein the AFM image displays no significant surface coverage (Fig. 1a). On the other hand, for the 5-hr sample, a relatively dense, thin layer is observed as shown in Fig. 1b. For the 20-hr and 24-hr samples, the particle (grain) structure becomes coarser and thicker, indicating that the colloidal particles in the precursor solution have contributed more to film formation (Fig. 1c and 1d).

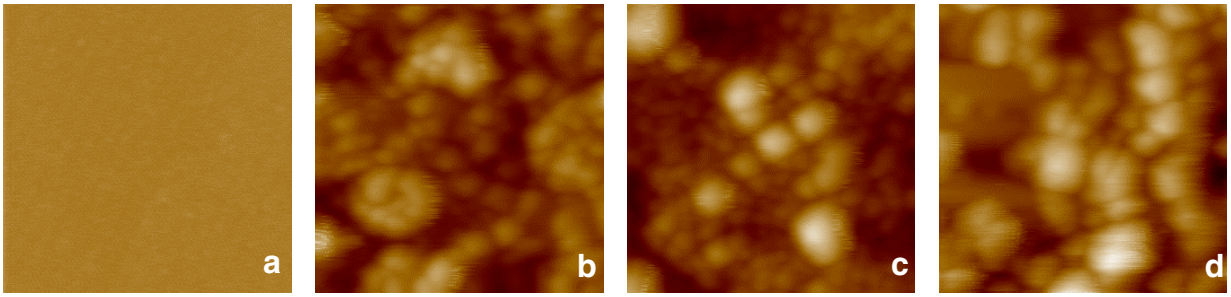

Figure 1. AFM images of four ceramic-coated samples taken out after different deposition time: (a) 0.5-hour, z-scan: 3.4nm, (b) 5-hours, z-scan: 91nm, (c) 20-hours, z-scan: 110nm, and (d) 24-hours, z-scan: 155nm. All images have xy-scan of 4μm x 4μm.

In fact, two film formation mechanisms have been suggested for such ZrO_2 film growth on the SAM template [6, 10]. The first mechanism is heterogeneous nucleation occurring at the SAM surface, thereby leading to directed growth of nuclei of the inorganic phase (biomimetic process). This mechanism results in strong adhesion between the ceramic film and the SAM, since the SAM surface functionality is designed to incorporate zirconia formation. One disadvantage of this process is that it may only deposit a relatively thin layer (less than 2-3 nm) [6]. The second mechanism involves homogeneous nucleation in solution, resulting in colloidal clusters by hydrolysis and condensation reactions of the dissolved species. These clusters are then attracted to the functional groups of the SAM by electrostatic interaction. This process, called bulk precipitation, can deposit much thicker films, whose structure uniformity is dependent on the size of the colloidal particles [11].

Mechanical properties of the ceramic films are compared in Fig. 2. For the 0.5-hr sample, both reduced Young's modulus and hardness are similar to those of Si. This is not unexpected since there is very little deposition on this sample, thus the sample surface can be either almost bare Si or very thin ceramic layer. There exists a large variation in the data of the 5-hr sample, whose upper limit of hardness is within bare Si range, while the lower limit is much smaller (about 2 GPa). A large variation in the mechanical properties must result from the indented areas that have a wide range of particle sizes or film thicknesses. The average modulus value of the 20-hr sample shows a similar modulus as compared to that of the 5-hr sample, although the average hardness value is reduced. For the 24-hr sample, both reduced Young's modulus and hardness values decrease, and the data scattering is also reduced. In summary, as immersion time increases, the surface becomes more covered with a zirconia film thus making it more uniform, and the particle or grain size increases.

Effects of the organic SAM on mechanical properties were also studied. For this purpose, the nanoindentation was impressed at the center of each particle and its thickness was measured by the cross-sectional profile of the AFM images. Two types of samples were studied; one is ZrO_2 film on PO-SAM coated Si (i.e., ZrO_2/PO-SAM/Si), and the other is ZrO_2 film on bare Si (i.e., ZrO_2/Si). For both samples, H and E_r decrease with the increasing film thickness. For the sample

with ZrO_2 film on bare Si, the average H is 1.9 GPa, and the average E_r is 81.4 GPa, whereas for the sample with ZrO_2 film on PO-SAM coated Si, the average H of the film is 1.7 GPa, and the average E_r is 50.4 GPa. It seems that the ZrO_2 film on PO-SAM coated Si is more compliant than that on bare Si while maintaining a similar hardness value. This result indicates that organic SAM acts as a compliant buffer layer, thus providing strain tolerance for the overlying hard ceramic film. It is also consistent with our previous FEA results [12].

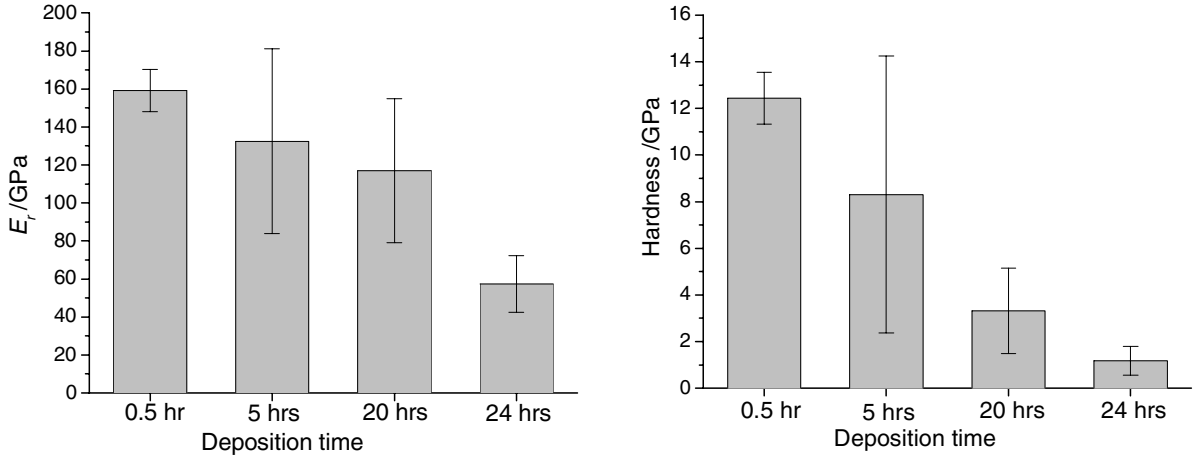

Figure 2. Mechanical properties of ZrO_2 films taken out at different ceramic deposition times. The error bars represent the standard deviation from the average value of the group (nine indentations or more).

The reduced Young's modulus (E_r) and hardness data obtained from the nanoindentation contain contributions from the substrate as well as from the film itself. For the film on substrate structure, a commonly suggested rule to get the "film only" properties by nanoindentation is to limit the indentation depth to less than 10% of the film thickness [13]. However, this rule is not applicable for ultra-thin films. Hence, in order to eliminate the substrate effect and get the "film only" Young's modulus (E_f), Nix's model [14] was applied as given by

$$\frac{1}{E_r} = \frac{1-\nu_i^{\,2}}{E_i} + \frac{1-\nu_f^{\,2}}{E_f}\left(1-e^{-\frac{\alpha(t-h)}{a}}\right) + \frac{1-\nu_s^{\,2}}{E_s}\left(e^{-\frac{\alpha(t-h)}{a}}\right) \tag{3}$$

where subscripts i, f, s represent indenter, film and substrate respectively, a is the square root of the projected contact area, t is the thickness of the film, h is the total indenter displacement, and α is a numerically determined scaling parameter that is a function of a/t and indenter geometries.

One example of the substrate effect is shown in Fig. 3. The results show that E_f of the ZrO_2 film calculated by the above Nix's model were much lower than E_f calculated from Eq. (1) due to the compliant thin film. In addition, there is little variation of E_f with film thickness after the data are corrected by this model. It indicates that particle size effect, or more accurately, film thickness effect observed before the model is applied is mainly caused by the substrate effect. Usually, larger particles are thicker, and have less substrate effect than do smaller particles.

To study the substrate effect more quantitatively, we applied Nix's model to four samples: a) trichlorosilane SAM on Si, b) ZrO_2 film on PO-SAM-coated Si, c) ZrO_2 film on Si, and d) SiO_2 film on Si. The sequence of mechanical properties from compliant to stiff film is: trichlorosilane SAM < ZrO_2 film* (with a PO-SAM) < ZrO_2 film* < SiO_2 film (*from *in-situ* prepared in solution). Fig. 4 shows the relationship between substrate effect and normalized Young's

modulus of the film (E_f / E_{Si}), where substrate effect is represented by ($E_r - E_f$)/ E_r . Since trichlorosilane SAM is the most compliant film among them, it has the largest substrate effect which is close to 1.

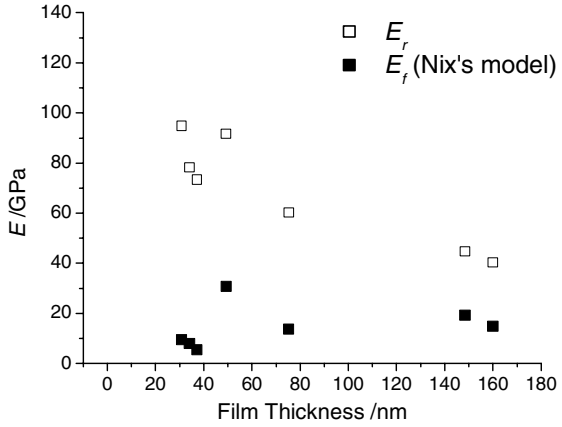

Figure 3. Reduced Young's modulus (E_r) and "film only" Young's modulus (E_f) of ceramic films on PO-SAM coated Si, as a function of film thickness.

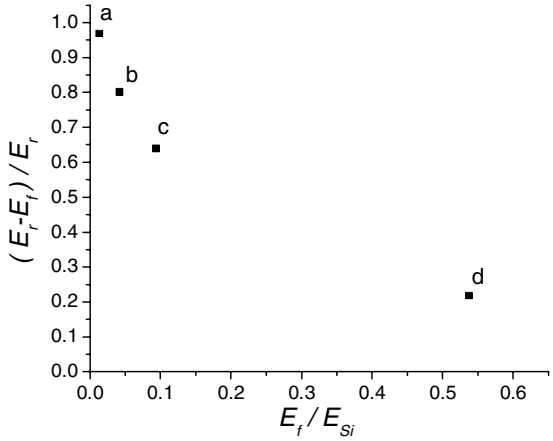

Figure 4. Substrate effect from 4 different thin films: a) trichlorosilane SAM on Si, b) ZrO_2 film on PO-SAM/Si, c) ZrO_2 film on Si, and d) SiO_2 film on Si. Indentation depth was 50% of the film thickness.

Both hardness and modulus of the zirconia films from the precursor solution were rather low as shown before. This may be due to nature of the film structure that contains both amorphous and crystalline phases at the time of deposition. This mixture in the film was confirmed by our TEM results [15]. In this case, the nanoindentation data can be influenced by the sandwiched amorphous phases. After high-temperature annealing (>1000°C), more amorphous phase was transformed to a tetragonal (*t*-) and monoclinic (*m*-) ZrO_2 phase [11]. Mechanical characterization of the annealed ceramic films, as shown in Fig. 5, indeed follows the structural evolution observed from XRD [11,12]. More mechanistic studies are currently underway to better understand the structure-mechanical property relation of the SAM-mediated ceramic films.

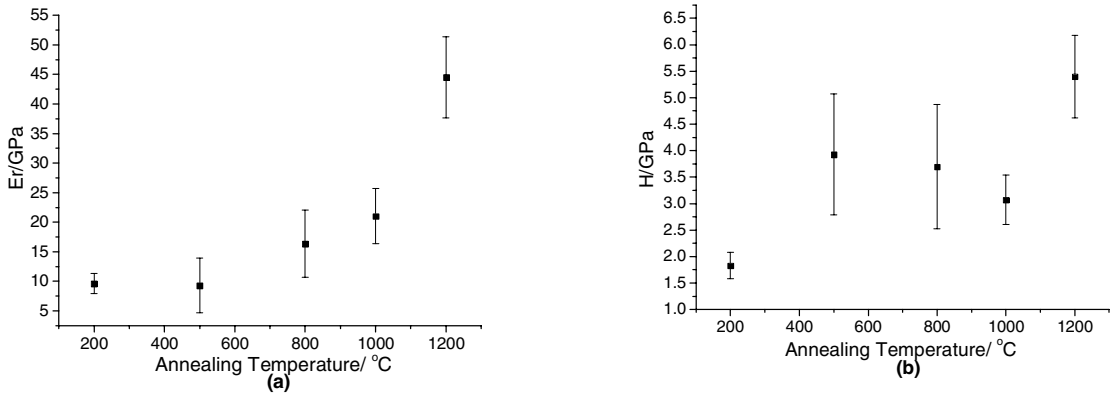

Figure 5. (a) Reduced Young's modulus and (b) hardness of ceramic film on PO-SAM coated Si after annealing at different temperatures. The error bars represent the standard deviation from the average value of the group (four indentations or more).

CONCLUSIONS

ZrO_2 films were deposited on silicon in zirconium sulfate/HCl solutions with the aid of self-assembled monolayer (SAM) at very low temperature (80°C). Mechanical properties of the ceramic/SAM bilayer structure were studied via nanoindentation. The results showed rather low hardness and modulus of the zirconia films. It was also observed that the bilayer structure has more compliance than a single layer film while losing no surface protection capability. Substrate effect was studied by analyzing nanoindentation data obtained from different film thicknesses using Nix's model. After excluding the substrate effect through this model, the mechanical properties almost showed a constant value independent of film thickness. High-temperature annealing of the zirconia films resulted in an increase in the mechanical properties due to more crystalline phase formed in the structure.

ACKNOWLEDGMENTS

This work was funded by Infotonics Technology Center Inc. (US DOE Grant #: DE-FG02-02ER63410.A000) and partially supported by Integrated Electronics Engineering Center (IEEC) of State University of New York at Binghamton. The authors would also like to thank Prof. S. Oliver and Dr. T. Salami for helping with synthesis and processing of SAM.

REFERENCES

1. U. Srinivasan, M. Houston, R. Howe, and T. Roger, *J. Microelectromechanical Systems*, **7**, 252-260 (1998).
2. A. R. Bishop and R. G. Nuzzo, *Curr. Opin. Col. Int. Sci.*, **1**, 127-136 (1996).
3. A. Ulman, *Chem. Re*v., **96**, 1533-1554 (1996).
4. S. W. Keller, H.-N. Kim, and T. E. Mallouk, *J. Am. Chem. Soc.*, **116**, 8817-8818 (1994).
5. G. M. Whitesides, *Sci. Amer.* Sept., **273**, 146-149 (1995).
6. M. Agarwal, M. R. De guire, and A. H. Heuer, *J. Am. Ceram. Soc.,* **80** (12), 2967 (1997).
7. J. Wang, S. Yang, X. Liu, S. Ren, F. Guan, and M. Chen, *Applied Surface Science*, **221**, 272 (2004).
8. V. V. Roddatis, D. S. Su, E. Beckmann, F. C. Jentoft, U. Braun, J. Krohnert, and R. Schlogl, *Surface and Coatings Technology*, **151 -152**, 63 (2002).
9. Q. Yang, K. Chitre, T. O. Salami, S. R. Oliver, and J. Cho, Paper No. IMECE2003-41700 in *Proceedings of IMECE,* **2** (ASME International Mechanical Engineering Congress and Exposition, Washington, D.C., 2003.), New York, NY, 2003.
10. J. Bill, R. C. Hoffmann, T. M. Fuchs, and F. Aldinger, *Z. Metallkd.*, **93**, 478 (2002).
11. K. Chitre, Q. Yang, T. O. Salami, S. R. Oliver, and J. Cho, in press, *J. Electro. Mater.* (2005).
12. Q. Yang, T. O Salami, K. Chitre, S. R. J. Oliver, and J. Cho, *MRS Proceedings*, **791**, 105-110 (2004).
13. W. C. Oliver and G. M. Pharr, *J. Mater. Res.*, **7** (6), 2765-2773 (1992).
14. R. Saha and W. D. Nix, *Acta Materialia*, **50**, 23–38 (2002).
15. G. Zhang and J. Cho, unpublished result (2004).